Available online at www.sciencedirect.com
ScienceDirect
Ceramics International 35 (2009) 797–802
CERAMICS INTERNATIONAL
www.elsevier.com/locate/ceramint

Shape dependence of corrosion kinetics of Si_3N_4 ceramics in acids

M. Herrmann *, J. Schilm

IKTS Fraunhofer Institute for Ceramic Technologies and Systems, Winterbergstr. 28, 01277 Dresden, Germany

Received 21 August 2007; received in revised form 21 January 2008; accepted 22 February 2008
Available online 4 July 2008

Abstract

The corrosion behaviour of Si_3N_4 ceramics with constant composition (Y_2O_3–Al_2O_3 additives) but of different shapes – plate, cylinder and ball – was investigated in 0.5 mol/l H_2SO_4 at 90 °C. The corrosion kinetics were measured using weight losses and thickness of the corrosion layers. The investigation showed that the corrosion depends on the shape of the samples. The differences in corrosion kinetics cannot be explained by the shrinking core mechanism. They are caused by different formation rates of the passivating SiO_2-rich layers in the corroded materials.

Keywords: C. Corrosion; Silicon nitride; Grain boundary phases

1. Introduction

Silicon nitride materials are one of the most prominent structural ceramics, and are applied in areas in which properties like high strength, fracture toughness, hardness and corrosion resistance are necessary, e.g. in ball bearings, cutting tools and parts in heat combustion engines. Beside silicon nitride grains, the sintered silicon nitride ceramics contain a grain boundary formed by the sintering additives and SiO_2 existing on the surface of the starting Si_3N_4 powder [1]. The corrosion resistance of Si_3N_4 materials in acids strongly depends on the composition of the grain boundary phase, especially on the SiO_2 content of the grain boundary phase [1–6]. The most intensive corrosion was observed in acids of medium concentration [3,7].

In HCl, HNO_3 and H_2SO_4 only the grain boundary phase in the triple junctions are subjected to corrosion attack whereas the Si_3N_4 grains and the thin grain boundary films between the grains remain unattacked. As a result a strong corrosion layer is formed still having a strength of 400–500 MPa [2–4]. The corrosion of the amorphous grain boundary can be described as a two-step process—leaching and dissolution of the network modifier (Y^{3+}, Al^{3+}) and destruction of the hydrated remaining glassy network. It was shown that Si_3N_4 ceramics with Y_2O_3–Al_2O_3 sintering additives show a passivation behaviour [2–5]. The passivation is caused by the formation of a passivating SiO_2 rich layer in the corroded triple junctions. The formation of this layer was observed when the concentration of the silicic acid (hydrated SiO_2; $xSiO_2{\cdot}nH_2O$) in the pores was high. The formation depends on the relative rate of the two processes—hydrolysis of the network and the condensation reaction of the silicic acid. A strong shift into the direction of condensation reactions results in the formation of large non-soluble aggregates, forming the protecting layers [2–6]. The corrosion processes are schematically shown in Fig. 1. Typically, these layers are only formed if the grain boundary is leached out several 100 μm in depth. If the diffusion rate of the dissolved silicic acid in the pores of the corroded layer is high in comparison to the dissolution rate, the formation of the passivating layer is retarded or does not take place at all. In ball-like samples the ratio of the diffusion rate in the corroded layer to the dissolution rate is higher than in the plates. This is caused by geometrical reasons and is known as the shrinking core effect which leads to a dilution of the leached components inside the corrosion layer (Fig. 2), Therefore, it could be assumed that the passivation is influenced by the shape of the ceramic component. Such investigations do not exist in the literature. That is why, the corrosion behaviour of Si_3N_4 ceramics with constant composition but of different shapes – plate, cylinder and ball – was investigated in 0.5 mol/l H_2SO_4 at 90 °C.

2. Experimental procedure

A Si_3N_4 material containing 6 wt.% Y_2O_3 and 4 wt.% Al_2O_3 was shaped by cold isostatic pressing as bars of the dimensions 24 mm × 24 mm × 65 mm and as balls with a diameter of

* Corresponding author. Tel.: +49 351 25 53 527; fax: +49 351 25 53 600.
E-mail address: mathias.herrmann@ikts.fraunhofer.de (M. Herrmann).

0272-8842/$34.00
doi:10.1016/j.ceramint.2008.02.021

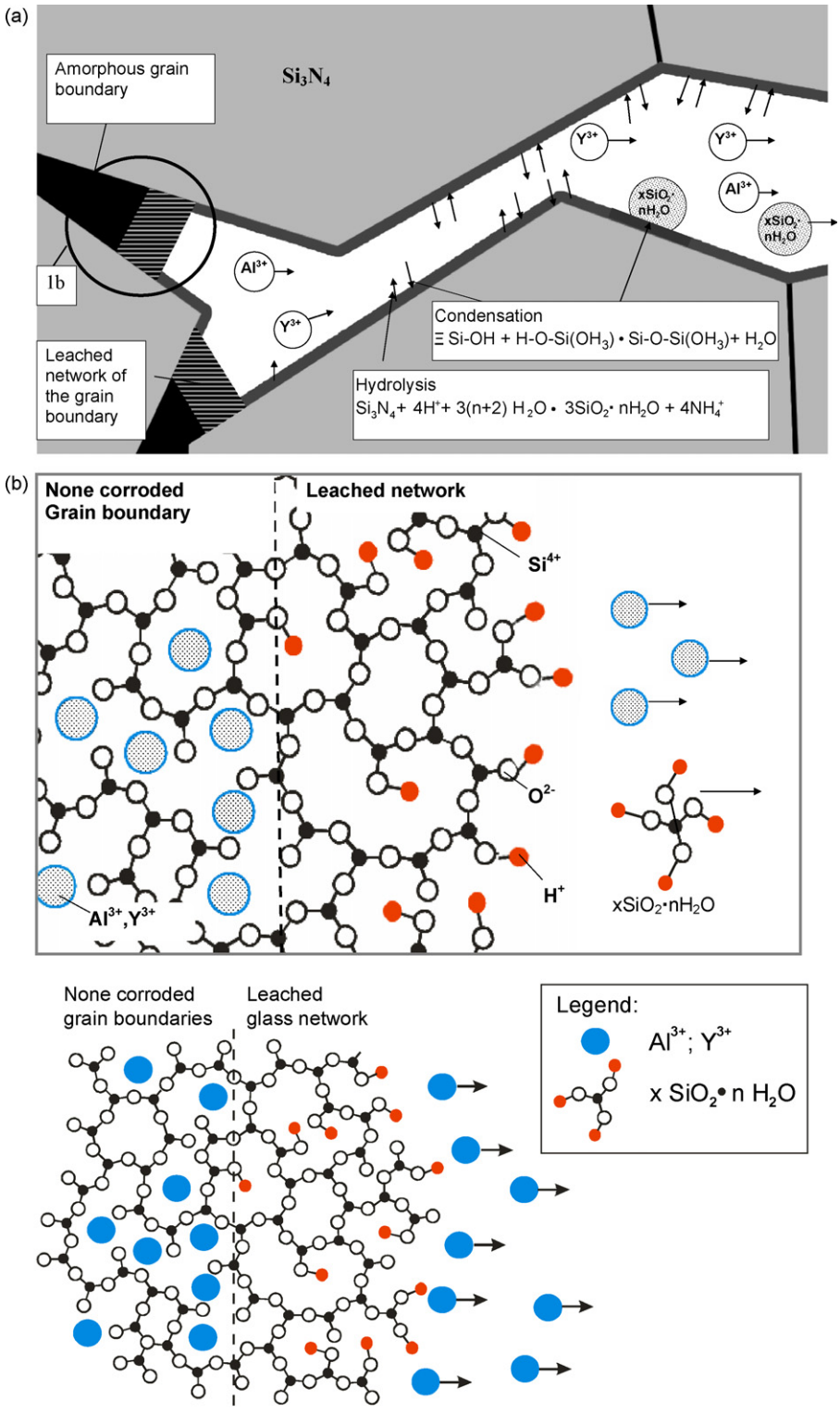

Fig. 1. Schematic illustration of the corrosion process.

4 mm. The samples were densified by gas pressure sintering at 1800 °C. To reduce the weight losses of the balls, which have a much higher surface to volume ratio, the sintering was conducted in a box made from Si_3N_4-rings and plates. The densities of the materials were higher than 99.9% of the theoretical density.

The weight losses of the sample were 0.59 wt.% for the bars and 0.65 wt.% for the balls. This weight loss is typical for sintering of silicon nitride. The decomposition takes place mostly in the near surface area. It is characterized by the reaction of SiO_2 with Si_3N_4 resulting in gaseous SiO and N_2. Therefore, the decomposition can result in a slightly reduced SiO_2 content in the material. The balls have a slightly higher weight loss due to the higher surface to volume ratio. After sintering the ciped bars were cut either into cylinders (∅

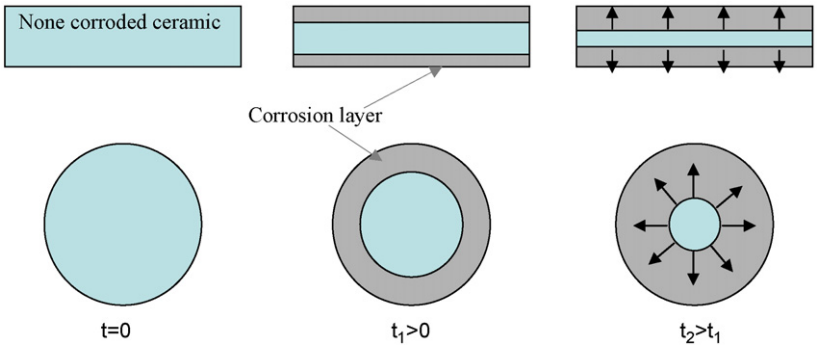

Fig. 2. Schematic illustration of the shrinking core model and the different ways of diffusion of the reaction product from the interface.

2.5 mm; length 45 mm) or into plates (16 mm × 16 mm × 2.5 mm). After finishing the balls had a diameter of 3.17 mm. Details of the preparation and methods of analysis are given in reference [3].

The corrosion tests were carried out in a 1.5 l teflon reaction vessel equipped with teflon sample holders. The solutions were continuously stirred and completely changed after a certain times in order to avoid a strong enrichment of dissolved glass components. A thermostat filled with silicone oil was used to heat the vessel. The requested temperature was maintained within a range of ±0.5 K. The standard preparation procedure before and after all corrosion experiments was to wash the samples in acetone for 10 min, to rinse them with deionised water, to dry them for ≥2 h at 150 °C and to weigh them on a microbalance (Δm = 0.01 mg) after a 2 h cooling period.

Cross sections of the corroded samples were investigated by optical microscopy and SEM. Corrosion indicators such as the thickness of corroded layers were evaluated by quantitative image analysis (Image Tool v3). The thickness of the corrosion layer was measured at cross sections as an average of the area of the layer. The typical errors of determination of the thicknesses were less than 15% for thicknesses of up to 50 μm, and less than 5% for thicker corrosion layers.

3. Results

The weight losses and the thicknesses of the corrosion layers of the different shaped samples are given in Fig. 3. Fig. 4 shows examples of the micrographs of the corroded cross sections. The cross sections show two sublayers in the corroded area. The outer layer is dark. The inner layer is lighter. In this paper we will call them in the paper inner and outer corrosion layer.

SEM and EDX investigations showed (Fig. 5) that the inner corrosion layer was more enriched in oxygen than the outer layer. In both layers no yttrium and only a strongly reduced amount of Al were detected. This indicates that Y_2O_3 and Al_2O_3 are leached out of the grain boundary by interdiffusion and ion exchange processes with protons from the acid. As a consequence it can be concluded that $xSiO_2{\cdot}nH_2O$ structures are formed inside the corroded triple junctions. A strong support for these assumptions come from TEM investigations of similar corroded samples which directly showed the formation of SiO_2 rich phases in the pores of the corroded samples [2]. During sintering Al is partially incorporated into the grains [3]. This amount of aluminum is not leached out, and can still be detected.

The mass losses during corrosion of the samples of different shapes are quite similar in the starting period. After a corrosion time of 30–40 h the slope of the curves (Fig. 3a) reduces. After 200 h the plates showed the highest weight losses, and the balls the lowest. However, the analysis has to take into account the different geometries of the corrosion interfaces, i.e. the so-called shrinking core effect [10,11]. The size of the interface between the corroded layer and the non-corroded material reduces for the cylinder and the ball, and is constant for the plates. Therefore, the amount of the grain boundary phase per given thickness of the corrosion layer, which can be leached out, reduces with increasing corrosion depth and corrosion time for the cylinder and the ball. The result of this shrinking core effect is that the weight loss reduces for the same change of thickness of the corrosion layers from the plate to the ball (this is illustrated by Fig. 2). If the corrosion mechanism is controlled by an interfacial reaction, the thickness of the corrosion layer would be the same for all three geometries, irrespective of the geometry. In fact this is the case within the starting period of the corrosion up to 30 h as Fig. 3b shows. The slightly higher corrosion rate of the spherical samples could be referred to the slightly

Table 1
Numerical results of the regression analysis of the corrosion data using a mixed reaction-controlled mechanism (equations after [9])

Geometry	Equation [9]	Coefficients/h	R^2
Plate	$t = 0.5 \cdot b \cdot \alpha^2 + a \cdot \alpha$	$a = -373 \pm 174$; $b = 2190 \pm 590$	0.840
Cylinder	$t = \left(1 - \sqrt[2]{1-\alpha}\right) \cdot a + (\alpha + (1-\alpha) \cdot \ln(1-\alpha)) \cdot \frac{b}{4}$	$a = -161 \pm 85$; $b = 1386 \pm 365$	0.908
Ball	$t = \left(1 - \sqrt[3]{1-\alpha}\right) \cdot a - \left(\frac{\alpha}{3} - 1 + \sqrt[3]{(1-\alpha)^2}\right) \cdot b$	$a = 1441 \pm 48$; $b = -1423 \pm 55$	0.996

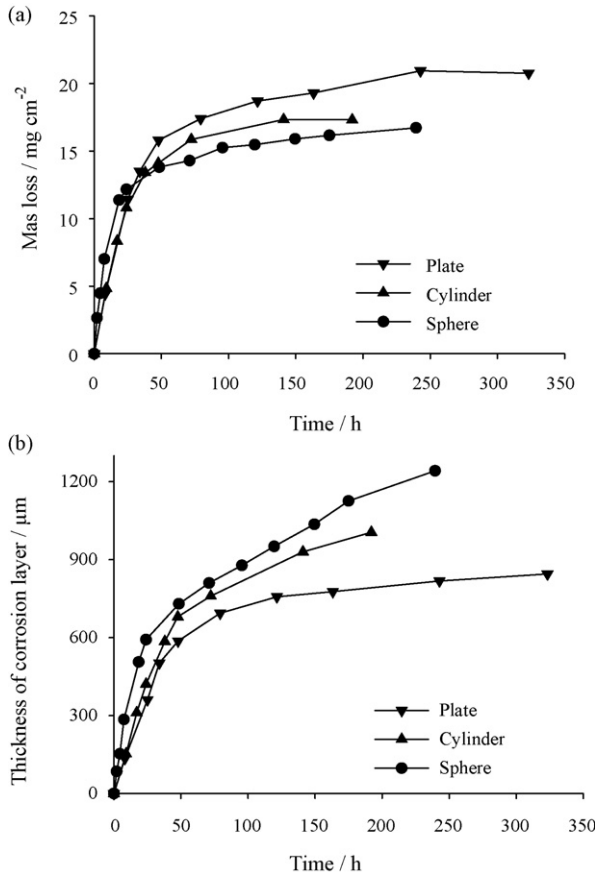

Fig. 3. Mass loss (a) and thickness of corroded layers (b) of the differently shaped samples (plate, cylinder and sphere) in 0.5 mol/l H_2SO_4 at 90 °C.

higher weight loss during sintering resulting in a little bit less stable grain boundary phase as in detail shown in references [2,3].

For the period after the initial 30 h of corrosion large differences in the thicknesses of the corrosion layers exist between the differently shaped samples. Whereas the corrosion layer thickness changes only slightly for the plate-like samples, the thickness of the corrosion layer increases for the cylindrical samples and even more for the ball-like samples with proceeding time of corrosion.

For the kinetic analysis and for the description of the kinetics the recalculation of the corrosion layer thickness into a degree of corrosion α is more convenient [10,11]. The degree of corrosion α is defined as

$$\alpha = \frac{V_{\text{corroded}}}{V_{\text{overall}}} \quad (1)$$

i.e. the ratio of corroded volume to total volume of the sample. The degrees of corrosion, recalculated from the original data, are given in Fig. 6 for the three samples. Additionally, the fitted curves according to a model that describes a mixed reaction control (overlapping of reaction and diffusion control) are shown. The results of the fits, which are given in Table 1, demonstrate that no reasonable fit is possible. For the ball-like samples the R^2 value (figure of merit of the regression) reaches nearly 1, indicating a good fit. However, also in this case the fit makes no sense, because one of the coefficients is negative. Such negative coefficient has no chemical meaning [10]. This is a strong indication that the changes of corrosion rate are not only caused by the change from reaction control to diffusion control, but also by the appearance of a different extent of passivation.

4. Discussion

The analysis of corrosion kinetics (Figs. 3 and 6) shows that the first period of corrosion can be described by a reaction-controlled mechanism. For a reaction-controlled corrosion the thickness of the reaction zone has to be proportional to the time over the entire corrosion process, irrespective of the sample's shape. The slope of the corrosion layer thickness/time curves is the same for all three shapes for corrosion times less than 30 h. This indicates an interface-controlled mechanism with the same rate constant for all samples. If the corrosion depth is low, the outward diffusion of the products of the corrosion of the grain boundary phase (Al^{3+}, Y^{3+} and $xSiO_2{\cdot}nH_2O$) is higher than the dissolution rate. The corroded layer therefore only consists of the strong skeleton of Si_3N_4 grains. The oxygen as well as the yttrium and aluminum content is low in this layer as the EDX measurements showed.

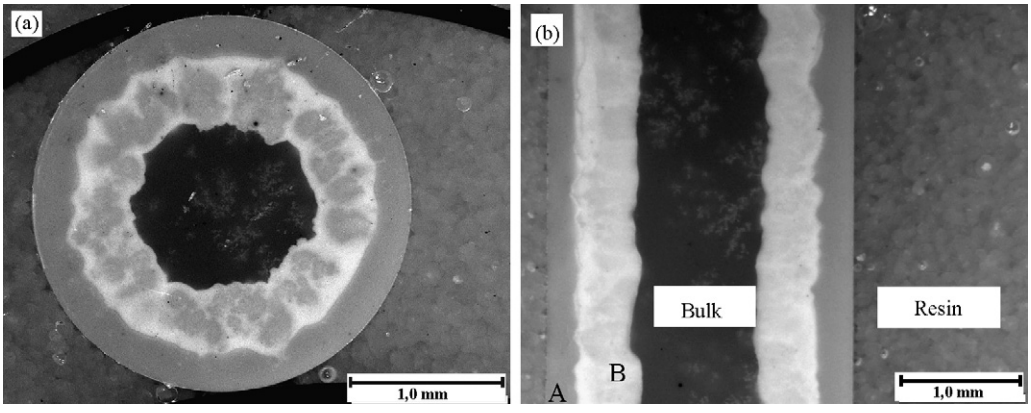

Fig. 4. Micrograph of the cross section of the cylinder after a corrosion time of 48 h (a), and a plate after a corrosion time of 122 h (b). In figure b the different areas are marked: A, outer corrosion layer; B, inner corrosion layer; Bulk, the non-corroded centre of the sample; Resin, resin from the mounting of the sample.

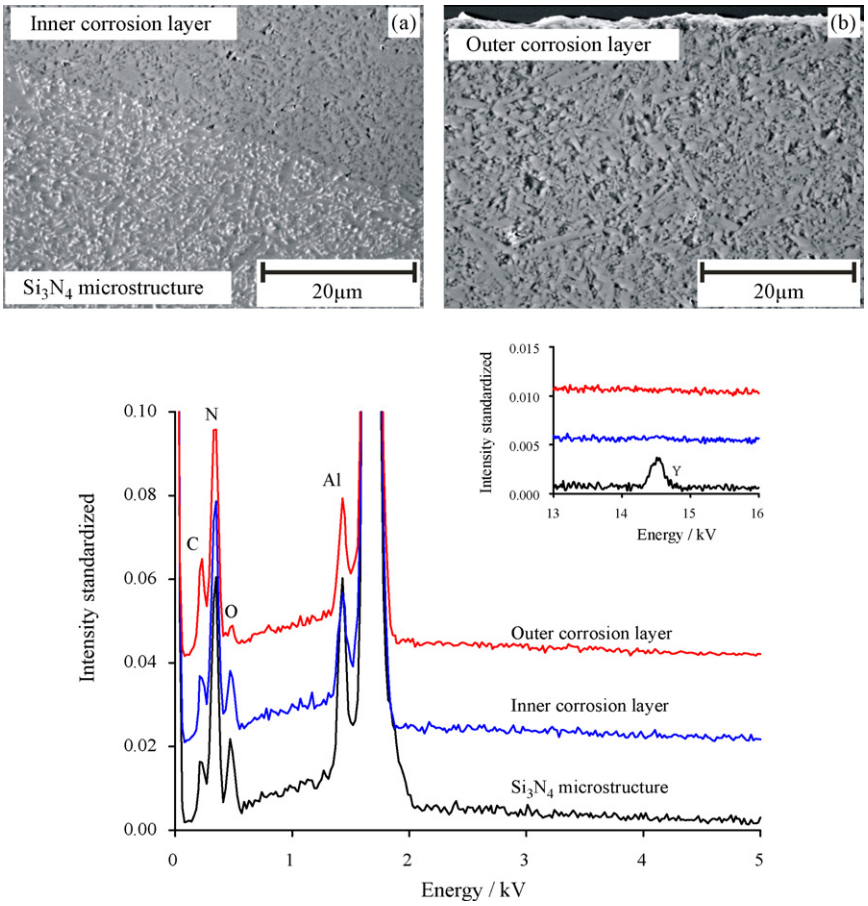

Fig. 5. SEM image and corresponding EDX signal for the inner and outer layer in the plate-like sample after a corrosion time of 216 h.

After a corrosion time of about 30 h (corresponding to thickness of the corrosion layer of 600–700 μm) the slope of the curves reduces (Fig. 3b). This indicates a change in the corrosion mechanism for all samples.

The strong reduction of the reaction rate after 50 h in the case of the plate can be explained by the formation of protection layers. A comparison of the EDX-peaks of the inner and outer layer in Fig. 5 strongly indicates a higher oxygen content in the inner layer than in the outer layer. Additionally a strong reduction of yttrium and aluminum is evident. Therefore, this protection layer (inner corrosion layer) is rich in silica. This layer is formed at the interface of corroded and non-corroded material and is called the inner corrosion layer. This was found also in previous investigations [2,3]. The formation of the corrosion layer is explained by the repolymerisation of soluble silicic acid $xSiO_2{\cdot}nH_2O$ species, formed as a reaction product inside the corrosion layer. Such processes are well known on surfaces of hydrated silica [9] being the reaction which converts soluble silicic acid to insoluble silica and can be summarized as:

$$2 \equiv Si{-}O{-}H \rightarrow \equiv Si{-}O{-}Si \equiv + H_2O \quad (2)$$

This is schematically shown in Fig. 1. This condensation reaction results in the reduction of the corrosion rate or even in passivation. The formation of such layers was observed by different methods for similar materials [2–7]. The reaction strongly depends on the concentration of the soluble silicic acid released from the grain boundary inside the corrosion layer. This reaction is of third order with respect to the monomeric silicic acid [8], and therefore the extent of repolymerisation, i.e. the formation of the passivating layer, is strongly referred to the ratio of the corrosion rate to the rate of transport of the soluble silicic acid from the corrosion interface to the surface of the sample. The faster outward diffusion of these species in the cylindrical and spherical samples, having a ratio of the higher

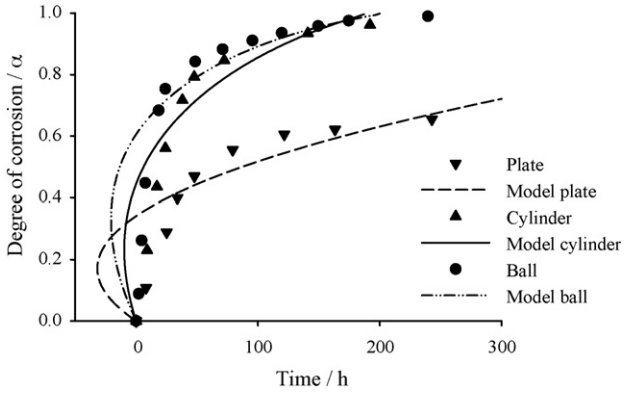

Fig. 6. Degree of corrosion as a function of corrosion time for the differently shaped samples. Additionally, the fitted curves for mixed reaction control (equations in Table 1) are shown.

accessible pore volume to the area of the reaction interface due to the shrinking core effect (see Fig. 2), results in the less pronounced formation of hydrated SiO_2 layers and less pronounced passivation of these samples. An equivalent explanation was given for the fact that SiO_2 rich corrosion layers were formed only in strong corroding materials at temperatures $>70\ ^\circ C$ and not at lower temperatures [3,4].

The consequence of this behaviour is that the corrosion of convex surfaces (edges, balls or tips) will be more intensive than that of flat surfaces. This has to be taken into account for the design of components operating in corrosive environments like ball bearings or valves for chemical apparatus. In the samples investigated here the passivation took place only at relatively high corrosion layer thicknesses (600–700 μm). But this passivation could take place at much lower thicknesses of the corrosion layer depending on the concentration of the acid, temperature or pre-treatment [3,7,8].

5. Summary

The corrosion behaviour of Si_3N_4 ceramics with constant composition (Y_2O_3–Al_2O_3 additives) but of different shapes – plate, cylinder and ball – was investigated in 0.5 mol/l H_2SO_4 at 90 °C. The investigation showed that the corrosion behaviour depends on the sample's shape. Samples with convex curved surfaces (ball, or cylinder) showed stronger corrosion than flat samples (plates). Measured differences in the corrosion kinetics cannot be described by the shrinking core mechanism, and are caused by the different extents of formation of a passivating SiO_2 rich layer in the corroded material. The formation of such layers is less pronounced in balls and cylinders than in plates.

References

[1] G. Petzow, M. Herrmann, Silicon nitride ceramics, Structure and Bonding, 102, Springer–Verlag, Berlin, Heidelberg, 2002, pp. 47–167.
[2] M. Herrmann, J. Schilm, W. Hermel, A. Michaelis, Corrosion behaviour of silicon nitride ceramics in aqueous solutions, J. Cer. Soc. Jap. 114 (11) (2006) 1069–1075.
[3] J. Schilm, W. Gruner, M. Herrmann, G. Michel, Corrosion of Si_3N_4-ceramics in aqueous solutions, J. Europ. Ceram. Soc. (2006) 3909–3917.
[4] M. Herrmann, J. Schilm, G. Michael, J. Meinhardt, R. Flegler, Corrosion of silicon nitride materials in acidic and basic solutions and under hydrothermal conditions, J. Europ. Ceram. Soc. 23 (2003) 585–594.
[5] J. Schilm, M. Herrmann, G. Michael, Kinetic study of the corrosion of silicon nitride materials in acids, J. Europ. Ceram. Soc. 23 (2003) 577–584.
[6] B. Seipel, K.G. Nickel, Corrosion of silicon nitride in aqueous acidic solutions: penetration monitoring, J. Europ. Cer. Soc. 23 (2003) 594–602.
[7] M. Shimada, T. Sato, Corrosion of silicon nitride ceramics in HF and HCl solutions, Ceram. Trans. Symp. 10 (1989) 355–364.
[8] B. Seipel, K.G. Nickel, Protection of silicon nitride ceramics against corrosion in acidic aqueous solutions by enforced internal passivation, ceramics international, Ceramics International 30 (2) (2004) 267–271.
[9] R.K. Iler, Chemistry of Silica (Russian Translation), Mir, Mockva 1982, 286 ff, 320.
[10] J.R. Frade, M. Cable, Numerical solutions for mixed control of powder reactions for spherical, cylindrical or planar particles, J. Am. Ceram. Soc. 78 (1995) 90–96.
[11] J.R. Frade, M. Cable, Theoretical solutions for mixed control of solid state reactions, J. Mat. Sci. 32 (1997) 2727–2733.